

Title	Improving production of volatile fatty acids and hydrogen from microalgae and rice residue: effects of physicochemical characteristics and mix ratios
Authors	Sun, Chihe;Xia, Ao;Liao, Qiang;Fu, Qian;Huang, Yun;Zhu, Xun;Wei, Pengfei;Lin, Richen;Murphy, Jerry D.
Publication date	2018-09-11
Original Citation	Sun, C., Xia, A., Liao, Q., Fu, Q., Huang, Y., Zhu, X., Wei, P., Lin, R. and Murphy, J. D. (2018) 'Improving production of volatile fatty acids and hydrogen from microalgae and rice residue: Effects of physicochemical characteristics and mix ratios', Applied Energy, 230, pp. 1082-1092. doi: 10.1016/j.apenergy.2018.09.066
Type of publication	Article (peer-reviewed)
Link to publisher's version	http://www.sciencedirect.com/science/article/pii/S0306261918313709 - 10.1016/j.apenergy.2018.09.066
Rights	© 2018 Elsevier Ltd. All rights reserved. This manuscript version is made available under the CC-BY-NC-ND 4.0 license - http://creativecommons.org/licenses/by-nc-nd/4.0/
Download date	2025-07-03 23:08:37
Item downloaded from	https://hdl.handle.net/10468/7004



UCC

University College Cork, Ireland
Coláiste na hOllscoile Corcaigh

**Improving production of volatile fatty acids and hydrogen from
microalgae and rice residue: Effects of physicochemical
characteristics and mix ratios**

Chihe Sun ^{a, b}, Ao Xia ^{*, a, b}, Qiang Liao ^{*, a, b}, Qian Fu ^{a, b}, Yun Huang ^{a, b}, Xun Zhu ^{a, b},
Pengfei Wei ^{a, b}, Richen Lin ^c and Jerry D. Murphy ^{c, d}

^a *Key Laboratory of Low-grade Energy Utilization Technologies and Systems, Chongqing
University, Ministry of Education, Chongqing 400044, China*

^b *Institute of Engineering Thermophysics, Chongqing University, Chongqing 400044, China*

^c *MaREI Centre, Environmental Research Institute, University College Cork, Cork, Ireland*

^d *School of Engineering, University College Cork, Cork, Ireland*

* Corresponding authors:

Email: aoxia@cqu.edu.cn (Ao Xia); lqzx@cqu.edu.cn (Qiang Liao).

Abstract

Dark fermentation may be hindered by insufficient bioavailable carbon and nitrogen sources as well as recalcitrant cell wall structures of substrates. Protein-rich microalgae and carbohydrate-rich rice residue with various mix ratios can optimise biohydrogen and volatile fatty acids production. Optimal pretreatment of the microalgae with 1% H₂SO₄ and the rice residue with 0.5% H₂SO₄ under hydrothermal heating (140 °C, 10 min) achieved reducing sugar yields of 187.3 mg/g volatile solids (VS) (hydrolysis efficiency: 54%) and 924.9 mg/g VS (hydrolysis efficiency: 100%), respectively. Multiscale physicochemical characterisations of solid hydrolytic residues confirmed considerable damage to both substrates. Co-fermentation of pretreated rice residue and microalgae at a mix ratio of 5:1 exhibited the maximum hydrogen yield of 201.8 mL/g VS, a 10.7-fold increase compared to mono-fermentation of pretreated microalgae. The mix ratio of 25:1 resulted in the highest carbon to volatile fatty acids conversion (96.8%), corresponding to a maximum energy conversion efficiency of 90.8%.

Keywords: Microalgae; Rice residue; Pretreatment; Physicochemical characteristics; Mix ratios; Co-fermentation.

1 Introduction

Dark fermentation (DF) is considered as a promising bioconversion technology, in which various types of biomass and organic wastes can be converted to volatile fatty acids (VFAs) and hydrogen by anaerobic microorganisms at relatively low temperature (35-55 °C) and ambient pressure [1, 2]. The large amounts of VFAs contained in the DF effluents provide valuable raw materials for the downstream microbial factories to produce biofuels (such as biomethane) and biochemicals (such as polyhydroxyalkanoate) [3]. Additionally, compared with energy-intensive hydrogen production methods (such as steam reforming of methane), hydrogen produced via DF is more sustainable and environmentally friendly [2]. Notably, the choice of substrates is the key factor to enhance VFAs and hydrogen production.

Microalgae are a promising biomass substrate due to their fast growth rate, superior CO₂ fixation capacity, and lack of any requirement for arable land for cultivation [4-6]. Notably, when microalgae are used as the single substrate during DF, the specific hydrogen yields are generally as low as 7.1-113.1 mL/g VS [7]. This is mainly caused by the following two reasons: (1) the high protein content (10%-84%) in microalgae with low biodegradable carbon sources [7] and, (2) the low release and hydrolysis of intracellular high-molecular compositions [8, 9].

Amino acids derived from proteolysis are essential nitrogen sources for microbial growth. Moderate amounts of amino acids can improve the bioactivity of hydrogen producing bacteria (HPB) and enhance the DF performance. However, amino acids are inefficient substrates for DF with negligible hydrogen production

(around 0.5 mL/g VS) [10]. Meanwhile, amino acids can be further hydrolysed to ammonia nitrogen ($\text{NH}_4^+\text{-N}$); excess proteins would ultimately cause the significant accumulation of $\text{NH}_4^+\text{-N}$, which may inhibit the physiological metabolism of HPB [11-13]. On account of this, co-fermentation of protein-rich microalgae and carbohydrate-rich biomass can increase the bioavailable carbon sources, thereby achieving efficient VFAs and hydrogen production [14]. Rice residue (RR), which is typically the dominant composition of food waste in China, is considered as a potential candidate because of its high biodegradability and high carbohydrate content. In 2015, the amount of rice wasted at the “dinner table” in China was around 4.5 Mt, equivalently to 30% of total food waste [15]. Co-fermentation of microalgae and RR not only can treat the environmental problem of food waste, but also can provide VFAs and carbon-free biohydrogen. However, to the best of our knowledge, such a process has yet to be reported.

High-molecular weight substrates in biomass (such as polysaccharides and proteins) are surrounded by a rigid cell wall structure that is hard for HPB to access and degrade [16, 17]. In order to release and hydrolyse the intracellular organic matter, the biomass cell wall should be disrupted prior to DF. Various pretreatments such as thermochemical, physical, and biological technologies have been employed to hydrolyse biomass [18]. Among them, hydrothermal acid pretreatment is considered as a simple and efficient method with a high hydrolysis rate of converting high-molecular weight substrates to low-molecular ones (such as glucose and amino acid) [7, 14, 19]. Notably, most of these previous studies just focused on the yield of

organic matter solubilisation, while the physicochemical characteristics of solid biomass hydrolytic residues were rarely investigated. Mendez et al. found that about 30% of carbohydrates and 45% of proteins still remained in the solid residues [19]; these organic materials can be also effectively used to produce VFAs and hydrogen via DF. Additionally, solid residues with different chemical composition can directly affect the bioaccessibility of biomass hydrolysates [20], and the changes of functional groups can be used to analyse fermentation inhibitors (such as furans and phenols) produced by pretreatment [21].

In this study, microalgae *Chlorella pyrenoidosa* (CP) and RR separately pretreated by diluted sulphuric acid catalysis under a hydrothermal environment were used as mixed substrates to improve the performance of fermentative VFAs and hydrogen production. The objects of this study are to:

- Assess the effects of pretreatment parameters on the hydrolysis characteristics of microalgae and rice residue.
- Compare the changes of surface microstructures, thermal stability, chemical composition and functional groups between raw biomass and solid hydrolytic residues.
- Evaluate the effects of mix ratios of microalgae and rice residue on VFAs and hydrogen production during dark fermentation.
- Analyse the carbon conversion efficiency (CCE) and energy conversion efficiency (ECE) of dark fermentation.

2 Materials and methods

2.1. Substrates and inocula

RR was collected from a dining hall located in Chongqing University, China. The collected RR was washed with deionized water to remove the attached greases and then blended into pulp in a blender. RR pulp was stored in a refrigerator at $-20\text{ }^{\circ}\text{C}$ before use. CP powder was purchased from a microalgae production plant located in Shandong Province, China. The purchased CP powder was stored in a cool and dry place at room temperature before use. The characteristics of RR pulp and CP powder are outlined in Table 1.

HPB were sourced from a rural household digester in Chongqing, China. The original sludge was heated in an autoclave at $100\text{ }^{\circ}\text{C}$ for 30 min to inactivate methanogens and to obtain the spore-forming HPB. Subsequently, the spore-forming HPB were acclimatised 3 times (3 days each time interval) using a modified culture medium [22] at $35.0 \pm 0.5\text{ }^{\circ}\text{C}$ under an anaerobic environment. Total solids (TS) and VS of the activated HPB were determined as 106.21 and 61.56 g/kg fresh weight, respectively.

2.2. Pretreatment of substrates

The separate pretreatments of RR and CP were conducted in triplicate in a reaction kettle (QN-WCGF, Taikang, China) with a working volume of 50 mL. The effects of reaction parameters, including reaction temperature (80-180 $^{\circ}\text{C}$), concentration of sulphuric acid (0-5%), reaction time (0-120 min), and substrate concentration (12.5-150 g TS/L), on the yields of organic matter solubilisation including solubilised

chemical oxygen demand (COD), carbohydrates, proteins, and reducing sugars in the supernatants of hydrolysates were evaluated. Raw RR and CP without any pretreatments were also assessed. During the experimental process, the time at which the desired temperature was reached in the reaction kettle was considered as time 0. The substrate concentration was defined as the required substrate level of RR or CP to 50 mL deionized water. After pretreatment, the hydrolysates composed of solubilised matters and solid residues were neutralised using 3 M NaOH and HCl solutions, and transferred to 50 mL centrifuge tubes, and then stored at $-20\text{ }^{\circ}\text{C}$ before use.

2.3. *Dark fermentation*

DF was performed in triplicate in the 500 mL glass fermenters. The working volume of each fermenter was 300 mL. Before the DF trials, the optimal reaction conditions obtained from separate pretreatments of RR ($140\text{ }^{\circ}\text{C}$, 10 min, 50 g TS/L, 0.5% H_2SO_4) and CP ($140\text{ }^{\circ}\text{C}$, 10 min, 75 g TS/L, 1% H_2SO_4) were set as the experimental parameters. To analyse the effects of the mix ratios of substrates on fermentative hydrogen production, 3.0 g VS of hydrolysates at various mix ratios were used for DF trials. The mixes on the basis of VS ratios of RR to CP were 0:1 (pure CP), 1:1, 2.5:1, 5:1, 25:1, and 1:0 (pure RR), respectively; these correspond to C/N molar ratios of 6.35, 10.01, 13.74, 17.61, 25.67, and 29.81, respectively. A certain amount of deionized water was added to maintain an overall volume of 270 mL. Subsequently, 30 mL of activated HPB was added to each fermenter.

The initial pH values were adjusted to 6.5 ± 0.1 using 3 M NaOH and HCl solutions. All the glass fermenters were sealed with butyl rubber stoppers and were

purged with nitrogen for 5 min to ensure an anaerobic environment. They were then placed in a thermostatic water bath at 35.0 ± 0.5 °C for 72 h. The pH values were adjusted to 6.5 ± 0.1 at a time interval of 6 h or 12 h using 3 M NaOH and HCl solutions. The produced gases were released from the headspace of fermenters, and were collected in the graduated gas collectors, and then were recorded at a time interval of 6 h or 12 h. The barrier liquid in these gas collectors was saturated sodium chloride solution (pH 2) with methyl orange as the indicator [23]. A blank group only containing inocula and a control group separately using raw RR and CP as single substrate were also operated under the same experimental conditions.

2.4. Analytical methods

The technological processes and analytical parameters of co-fermentation from RR and CP are shown in Fig. 1. The contents of moisture, TS, VS, and ash were measured according to the Standard Methods 2540 G [24]. The contents of carbohydrates, reducing sugars, and proteins were determined as described in previous studies [25, 26]. A spectrophotometer (Hach DR3900, USA) coupled with a heating digestion unit (Hach DRB200, USA) was used to measure COD. An elemental analyser (Vario MACRO cube, Elementar, Germany) was used to analyse the contents of C, H, N, and S. The remaining content of VS was assumed as O. The pH value was analysed by a portable pH meter (F2, METTLER TOLEDO, Switzerland). The differences of biomass surface microstructures before and after pretreatment were observed by a field emission scanning electron microscope (SEM) (Zeiss Auriga, Germany). The changes of biomass thermal stabilities before and after pretreatment were evaluated by

a derivative thermogravimetric (DTG) analyser (DTG-60H, Shimadzu, Japan). The changes of chemical composition and functional groups were assessed by a Fourier transform infrared spectroscopy (FTIR) analyser (Nicolet iS5, ThermoFisher, USA).

Hydrogen and carbon dioxide were determined by a gas chromatograph (GC) (Trace 1300, ThermoFisher, USA) equipped with a micro-packed column (ShinCarbon ST Columns, 2 m, OD 1/16, ID 1.0 mm, Mesh 100/120) and a thermal conductivity detector (TCD). The composition of VFAs including acetic acid, propionic acid, butyric acid, and caproic acid in the DF effluents were analysed using another GC (Agilent 7890B, USA) equipped with a polar capillary column (Agilent DB-FFAP Column, 30 m × 0.25 mm × 0.25 μm) and a flame ionization detector (FID).

All the experimental trials and measurements were conducted in triplicate, and the results were expressed as the average (\pm standard deviation).

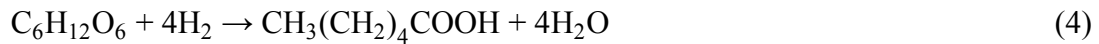
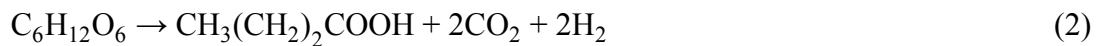
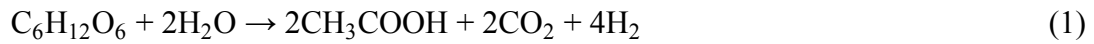
2.5. Calculation

The contents (mg/g VS) of total and solubilised organic matters in the original biomass and the supernatants of hydrolysates were calculated using the ratios of the weight of these materials (mg VS) to the initial substrate weight (g VS). The hydrolysis efficiency of carbohydrates (%) was defined as the ratio of the reducing sugar content in the supernatants of hydrolysates (mg/g VS) to the total carbohydrate content in the original biomass (mg/g VS). The specific hydrogen yield (mL/g VS) was defined as the ratio of the final cumulative hydrogen volume (mL) to the original substrate weight (g VS); the final cumulative hydrogen volume was calculated based

on the volume of total gases (normalized to 0 °C and 1 atm) and content of hydrogen both in the fermenter headspace and gas collector at each time interval [22].

The specific hydrogen yield was simulated using a modified Gompertz equation [27], and the kinetic parameters (H_m , maximum production potential, mL/g VS; R_m , peak rate, mL/g VS/h; T_m , peak time, h; λ , lag-phase time, h) were calculated through Origin software. The final cumulative concentrations of VFAs (mM) in the DF effluents were used to assess the fermentation physiological metabolism. To eliminate the effects of inocula, the data were calculated by subtracting the concentrations in the experimental groups from these in the blank group.

The hydrogen discrepancy factor (HDF, %) was defined as the differences between the theoretical and experimental hydrogen production [28]. The relationship of VFAs and hydrogen produced from glucose was obtained by the stoichiometric equations, as shown in Eqs. (1)-(4) [29, 30].



Overall, the theoretical hydrogen production was calculated based on Eq. (5), while the hydrogen discrepancy factor was calculated based on Eq. (6) [28].

$$\text{H}_2^{\text{T}} (\text{mol}) = \text{H}_2^{\text{A}} + \text{H}_2^{\text{B}} - \text{H}_2^{\text{P}} - \text{H}_2^{\text{C}} \quad (5)$$

$$\text{HDF} (\%) = | (\text{H}_2^{\text{T}} - \text{H}_2^{\text{Exp}}) / \text{H}_2^{\text{T}} | \times 100 \quad (6)$$

where H_2^{T} and H_2^{Exp} represent the theoretical and experimental total hydrogen

production, respectively. H_2^A and H_2^B represent the theoretical hydrogen production from acetic acid (Eq. (1)) and butyric acid (Eq. (2)) pathways, respectively. H_2^P and H_2^C represent the theoretical hydrogen consumption from propionic acid (Eq. (3)) and caproic acid (Eq. (4)) pathways, respectively.

The CCE (%) was calculated based on the ratio of the total carbon yield (g) of produced VFAs and carbon dioxide to the total carbon (g) of the original substrates. Meanwhile, the ECE (%) was calculated using the ratio of the total energy value (kJ) of produced VFAs and hydrogen to the total energy value (kJ) of the original substrates. The higher heating values of acetic acid (874 kJ/mol), propionic acid (1527 kJ/mol), butyric acid (2184 kJ/mol), caproic acid (3492 kJ/g VS), and hydrogen (286 kJ/mol) were based on previous studies [14, 31]. The heating values (kJ/g VS) of RR and CP were calculated based on the determined VS percentages of C, H, O, N, and S using the Mendeleev formula as shown in Eq. (7).

$$\text{Heating value (kJ/g VS)} = 0.33858C + 1.254H - 0.10868(O - S) \quad (7)$$

3 Results and discussion

3.1. Effects of pretreatment parameters on organic matter solubilisation

3.1.1. Reaction temperature

High concentrations of amino acids and sugars are very reactive under hydrothermal conditions; this may result in generation of a quantity of fermentative inhibitors via the Maillard reaction [19, 32, 33]. Therefore, the substrates of carbohydrate-rich RR and protein-rich CP were separately pretreated in this study. The effects of reaction

temperature on the yields of organic matter solubilisation are as shown in Figs. 2a and e. Experiments were conducted at a H₂SO₄ concentration of 1% (v/v) for 10 min by separately adding 50 g TS/L substrates of RR and CP.

When the reaction temperature was set as 80 °C, the solubilised COD yields of RR and CP were only 196.8 and 216.8 mg/g VS, respectively. This indicated that a low temperature could not provide enough energy to disrupt the biomass structure, thereby only releasing slight amounts of intracellular organic matters. The reducing sugar yields of RR (16.3 mg/g VS) and CP (15.4 mg/g VS) were also quite low, which may lead to a poor DF performance [31].

When the reaction temperature increased to 140 °C, the solubilised COD yields of RR and CP significantly increased to 1010.9 and 713.9 mg/g VS, respectively. Given the original COD contents of RR (1124.6 mg/g VS) and CP (1439.6 mg/g VS), as shown in Table 1, around 90% of organic matters in RR was released to the hydrolysates, whereas that of CP was only around 50%. RR could be more easily disrupted compared with CP, which has a complex cell wall structure. Additionally, the reducing sugar yields of RR and CP significantly increased to 915.9 and 200.3 mg/g VS, respectively. This suggested that a significant increase in temperature could enhance the hydrolysis of polysaccharides. When the reaction temperature further increased to 180 °C, the reducing sugar yields of RR and CP gradually decreased to 422.3 and 120.5 mg/g VS, respectively. This was attributed to the subsequent decomposition of sugars.

The main type of carbohydrates in RR and CP are starch [34]; they can be

effectively hydrolysed into reducing sugars (such as maltose and glucose) due to the fracture of glycosidic bonds. However, these low-molecular sugars would further break down into other by-products such as 5-hydroxymethylfurfural, formic acid, and levulinic acid at a high temperature [35-37], resulting in a decrease of reducing sugar yield. Compared with polysaccharide, the major components of protein are amino acids that are linked together by peptide bonds. Toor et al. found that peptide bonds were more stable than glycosidic bonds, and the hydrolysis rate of protein was quite slow at temperatures below 230 °C [38]. Thus, there was no significant downward trend in the solubilised protein yields of RR (from 102.2 to 111.4 mg/g VS) and CP (from 316.5 to 337.5 mg/g VS) when the reaction temperature increased from 140 to 180 °C. Since reducing sugars can be readily used by HPB to produce hydrogen and VFAs, the reaction temperature of RR and CP corresponding to the maximum reducing sugar yields was set at 140 °C in the following trials.

3.1.2. H₂SO₄ concentration

Figs. 2b and f depict the changes of organic matter solubilisation with various acid concentrations. Experiments were conducted at 140 °C for 10 min by separately adding 50 g TS/L substrates of RR and CP.

Compared with raw biomass, the solubilised COD yield of RR increased from 26.3 to 806.1 mg/g VS after hydrothermal pretreatment (acid concentration: 0%), while that of CP only increased from 121.5 to 249.7 mg/g VS. This result illustrated that the cell wall structure of CP could not be completely disrupted without adding diluted sulphuric acid; most of the intracellular organic matters was still in the

hydrolytic biomass residues. Although the solubilised carbohydrate yield of RR significantly increased from 4.2 to 600.5 mg/g VS, the reducing sugar yield only increased from 1.9 to 32.3 mg/g VS. Such a process would not convert the high-molecular matters (such as polysaccharides) to low-molecular ones (such as glucose), suggesting a low hydrogen yield [14].

When the acid concentration increased from 0.2% to 0.5%, the reducing sugar yield of RR significantly increased from 559.5 to 924.9 mg/g VS, and that of CP increased from 35.5 to 92.5 mg/g VS. The addition of diluted sulphuric acid in the hydrothermal pretreatment could improve the hydrolysis of polysaccharides [39]. Notably, the changing trends of these two substrates at a relative high acid concentration (more than 1%) were different. The reducing sugar yield of RR slightly decreased to 897.1 mg/g VS as the acid concentration increased to 1.5%; further increasing the acid concentration to 5% showed an apparent pick-up from 1088.4 to 1238.0 mg/g VS, which greatly exceeded the solubilised carbohydrate yield (804.4 mg/g VS). However, the reducing sugar yield of CP kept increasing from 200.3 to 235.8 mg/g VS when the acid concentration increased from 1% to 5%.

The differences were attributed to the different composition and contents of carbohydrates in RR (913.8 mg/g VS) and CP (347.9 mg/g VS), as shown in Table 1. In this study, reducing sugars were measured by 3,5-dinitrosalicylic acid (DNS method), which is considered as a chemical coloured reaction [40]. The reducing sugar yield is related to the absorbance of the solution. When carbohydrate-rich RR underwent hydrothermal pretreatment under a high dilute acid concentration (more

than 2%), the high amounts of coloured by-products (such as furfural and melanoidin) produced by Maillard reactions and self-decomposition of sugars affected the test performance [33, 41]. Additionally, Maillard products may possess the reductive groups such as free aldehyde and ketone groups. Although glucose could be self-decomposed into various by-products [33], some of these by-products may still have reduction properties. Based on this, excess reducing sugars detected in the hydrolysates of RR was also caused by the formation of these reductive substances. Overall, the optimal acid concentrations of RR and CP were set as 0.5% and 1%, respectively, to achieve high reducing sugar yields and minimise the acid use in the following trials.

3.1.3. Reaction time

The effects of reaction time on the yields of organic matter solubilisation are as shown in Figs. 2c and g. Experiments were conducted at 140 °C by separately adding 50 g TS/L substrates of RR and CP. The H₂SO₄ concentrations (v/v) for RR and CP were 0.5% and 1%, respectively.

A large quantity of solubilised organic matters had been already obtained during the heating process (0 min of reaction time). Compared with raw biomass, the solubilised COD yields of RR increased from 26.3 to 997.9 mg/g VS, and that of CP increased from 121.5 to 540.7 mg/g VS. Even so, the reducing sugar yields of RR (369.9 mg/g VS) and CP (86.2 mg/g VS) were still low. When the reaction time increased to 10 min, the reducing sugar yields of RR and CP significantly increased to 924.9 and 200.3 mg/g VS, respectively. These results suggested that polysaccharides

could not be fully hydrolysed without sufficient reaction time. When the reaction time increased from 10 to 60 min, the reducing sugar yields of RR (910.3 mg/g VS) and CP (206.1 mg/g VS) were slightly changed, indicating that biomass hydrolysis was nearly complete in 10 min.

Further increasing the reaction time to 120 min caused the subsequent decomposition of sugars, thereby resulting in lower reducing sugar yields of RR (856.5 mg/g VS) and CP (145.2 mg/g VS). Such a phenomenon was not found in the process of proteolysis. When the reaction time increased from 0 to 120 min, the solubilised protein yield of RR kept increasing from 66.4 to 121.4 mg/g VS, and that of CP kept increasing from 225.8 to 345.4 mg/g VS. It further confirmed that the peptide bonds in protein were more difficult to disrupt than the glycosidic bonds in carbohydrates. Overall, the optimal reaction time of RR and CP was set as 10 minutes, to achieve high reducing sugar yields with minimal energy input in the following trials.

3.1.4. Substrate concentration

The effects of substrate concentration on the yields of organic matter solubilisation are as shown in Figs. 2d and h. Experiments were conducted at 140 °C for 10 min by separately adding the required substrate level of RR and CP to 50 mL diluted acid solution. The H₂SO₄ concentrations (v/v) for RR and CP were 0.5% and 1%, respectively.

As the biomass substrate concentration increased from 12.5 to 150 g TS/L, the solubilised COD yield of RR sharply decreased from 1153.5 to 695.7 mg/g VS, and

that of CP significantly decreased from 930.6 to 500.6 mg/g VS. The yields of solubilised carbohydrates, proteins, and reducing sugars of RR and CP also showed a continuous decline. Since the working volume of the reaction kettle used for pretreatment was constant (50 mL), the addition of excess biomass would cause poor heat and mass transfer in the reactor. Insufficient sulphuric acid was another major factor that hindered the biomass catalytic hydrolysis. Overall, the optimal substrate concentrations of RR and CP were set as 50 g TS/L and 75 g TS/L, respectively, to achieve high reducing sugar yields with high biomass pretreatment capacity and low acid inputs per unit biomass (VS) in the following trials.

3.2. Comparison of physicochemical characteristics of solid residues

3.2.1. Surface microstructure analysis

The changes of biomass surface microstructures before and after pretreatment are shown in Fig. 3. Blocky organic fragments with various sizes were observed in raw RR (Fig. 3a). When raw RR was hydrothermally pretreated (without the addition of acid), these clumps were broken up and formed relatively small adhesive granules due to the gelatinization of starch (Fig. 3b). When diluted sulphuric acid (at 0.5% concentration) was employed in hydrothermal pretreatment, RR could be effectively disrupted into pieces (Fig. 3c). Spherical cells with no signs of pitting or damage were presented in the raw CP (Fig. 3d). After hydrothermal pretreatment, a few cells were distorted and collapsed, while most of them were still intact (Fig. 3e). Diluted sulphuric acid (at 1% concentration) could also completely disrupt the structure of CP cells under hydrothermal environment, and only very small particles at nanoscale

sizes were observed (Fig. 3f). Most importantly, these porous nanoparticles of CP increased the specific surface area of hydrolytic residues; efficient contact between organic matters and HPB may improve the DF performance [20, 42].

3.2.2. *Fourier transform infrared spectroscopy analysis*

The characteristics of functional groups shown in the FTIR spectra (Fig. 4) were used to distinguish the chemical differences among RR and CP before and after pretreatment. The broadest band in the range of 3600-3000 cm^{-1} was ascribed to —OH stretching vibrations associated with internal water [42]. This band presented an asymmetry caused by the amide I of proteins (N—H stretching vibrations at around 3285 cm^{-1}) [21, 43]. The asymmetry degree was positively related with the severity of pretreatment conditions. Whilst, the increase of asymmetry degree indicated excess release of proteins, which may cause a longer lag phase in DF [21]. The asymmetrical and symmetrical C—H stretching vibrations from aliphatic methylene groups at around 2925 and 2855 cm^{-1} were attributed to fatty acids of lipids [20]. The relative intensities of these two bands both increased after pretreatment due to the increase of surface exposure of lipids. Additionally, the stronger relative intensities of the bands at around 3445, 2925, and 2855 cm^{-1} in CP resulted in higher protein and lipid contents than RR.

The C=O stretching, C—N stretching, and N—H bending vibrations observed at around 1650, 1540, and 1200-1360 cm^{-1} were derived from amide I, amide II, and amide III of proteins, respectively [20, 21, 44]. After hydrothermal acid pretreatment, the increases of these bands in CP and RR indicated that the addition of dilute acid

could significantly disrupt the biomass structure and enhance the release of intracellular proteins. Moreover, the stronger relative intensities of these bands in CP further confirmed that the original content of proteins in CP was much higher than RR. Notably, compounds derived from Maillard reactions (C=N stretching vibrations at around 1647 and 1607-1463 cm^{-1}) impacted the intensities and positions of these bands [45, 46]. Mendez et al. reported that Maillard reactions could be strongly affected by the amino acid to sugar ratio [19]. As for these reasons, the relative intensities of the bands in the range of 1650-1400 cm^{-1} in the solid residues of CP obviously increased compared with RR after hydrothermal acid pretreatment. The accumulation of Maillard products (such as pyrazines, pyridines, ketones, and aldehydes) would inhibit the biological activities of HPB, thereby leading to a low hydrogen yield. Thus, co-fermentation of RR and CP would mitigation such an adverse situation.

Bands in the range of 1190-900 cm^{-1} in RR were assigned to C—O, C—OH, and C—C stretching vibrations derived from polysaccharides and phosphodiesteres, whereas the huge bands in the range of 1170-1000 cm^{-1} in CP were caused by mineral compounds (ash) [42]. Overall, compared with raw and hydrothermal pretreated biomass, the process of acid pretreatment completely disrupted the structures of RR and CP cells, which intensified the exposure of organic matters and further promoted the infrared absorption of corresponding functional groups.

3.2.3. Derivative thermogravimetric analysis

The DTG profiles obtained from RR and CP before and after pretreatment are as

shown in Fig. 5. Thermal weight losses of RR and CP comprised three stages [21, 47, 48]: (i) Release of free moisture ranged from 20 to 170 °C, (ii) Pyrolysis of high-molecular matters including carbohydrates, proteins, and lipids ranged from 170 to 375 °C, (iii) Further fracture of C—C and C—H bonds ranged from 400 to 900 °C. Significant differences between RR and CP in DTG profiles were observed in the second stage.

Since the chemical composition of RR (exceeding 90% starch in raw biomass) was less varied compared with CP (Table 1), the weight loss temperature region of RR was narrower than CP. Pretreatment conditions could also affect the biomass pyrolysis process. Compared with raw biomass, the changes in thermal weight loss of pretreated biomass were mainly caused by the different contents of organic matters contained in the biomass hydrolytic residues. In terms of hydrothermal acid pretreatment, the non-significant weight losses of hydrolytic residues of RR indicated that most of the organic matters (around 90%) was released into the liquid phase, as shown in Fig. 2d. Nevertheless, over 55% of organic matters of CP was still in the hydrolytic residues (Fig. 2h), resulting in few differences in the DTG curve. Notably, two peaks in the temperature range of 170-375 °C were reported for hydrothermal acid pretreatment, while only one peak was obtained from raw and hydrothermal pretreated biomass. The first special oxidation pattern, which occurred in the temperature range of 170-270 °C, illustrated the presence of labile fractions that could be easily degraded by HPB [21, 48].

3.3. Effects of biomass mix ratios on dark fermentation

3.3.1. Biohydrogen production

Figs. 6a and b show the effects of mix ratios of RR and CP on hydrogen yields and production rates. Since the reducing sugar content of raw RR was only 1.9 mg/g VS (Table 1), a long lag phase of around 48 h was observed during mono-fermentation of raw RR. Such a significant delay indicated that high-molecular weight starch could not be rapidly hydrolysed by HPB [14, 49]. However in the following 24 h, the specific hydrogen yield increased to 36.3 mL/g VS. With the increase of hydrolysis time, starch was gradually converted to low-molecular weight sugars and subsequently fermented to hydrogen.

When raw CP was used as the single fermentation substrate, almost no hydrogen was produced (1.2 mL/g VS). This result suggested that the compact cell structure of CP could not be effectively destroyed by HPB, thereby leading to a poor bioaccessibility of the intracellular compounds. Meanwhile, the low content of solubilised proteins (30.3 mg/g VS) and carbohydrates (54.3 mg/g VS) in raw CP (Table 1) did not support the growth and metabolism of HPB [14]. After hydrothermal acid pretreatment, the contents of solubilised organic matters especially reducing sugars obviously increased. Even so, the specific hydrogen yield and production rate slightly increased to 19.0 mL/g VS and 2.1 mL/g VS/h, due to the high original protein content in CP (480.9 mg/g VS). Lay et al. reported that the hydrogen production potential of substrates rich in proteins were 20 times lower than that of substrates rich in carbohydrates [42, 50]. Excess mineral compounds contained in CP could also damage the enzymatic function and structure of HPB, thereby debilitating

the biodegradation of substrates [42, 51].

When pretreated RR and CP were co-fermented at the mix ratios of 1:1-5:1, the specific hydrogen yield increased from 94.2 to 201.8 mL/g VS, and the specific hydrogen production rate increased from 9.9 to 14.7 mL/g VS/h. Increasing the mix ratios of RR and CP resulted in a higher concentration of bioavailable carbon sources (e.g., reducing sugars), which would further enhance the DF performance [14]. When the mix ratio further increased to 25:1, the specific hydrogen yield slightly decreased to 201.5 mL/g VS, and the specific hydrogen production rate significantly decreased to 11.1 mL/g VS/h. Mono-fermentation of RR decreased the concentration of nitrogen sources; the insufficient nitrogen sources hindered the growth and bioactivity of HPB [52].

Table 2 depicts the kinetic parameters of fermentative hydrogen production from pretreated RR and CP. The maximum hydrogen production potential of 200.5 mL/g VS and hydrogen production peak rate of 16.0 mL/g VS/h were both obtained at the mix ratio of 5:1, which was consistent with the experimental data.

3.3.2. Volatile fatty acids production

As shown in Table 3, the final cumulative VFAs in the DF effluents mainly contained abundant acetic acid (7.9-33.3 mM) and butyric acid (2.6-41.2 mM), and trace amounts of propionic acid (0.7-3.2 mM) and caproic acid (0.1-2.9 mM). In terms of mono-fermentation of raw RR, as well as raw and pretreated CP, the total VFAs concentrations were only 11.1, 13.3, and 25.9 mM, respectively; these relatively low VFAs concentrations further confirmed that the growth and metabolism of HPB were

hindered by insufficient bioavailable carbon sources. In terms of co-fermentation of pretreated RR and CP at the mix ratios of 1:1-25:1, the total VFAs concentration increased from 44.5 to 78.3 mM, indicating that the inhibition of bioavailable carbon sources were gradually mitigated. Meanwhile, the high utilisation efficiencies of reducing sugars (97.4%-99.5%) illustrated that most of hydrolysed carbohydrates were effectively utilised.

Based on the production of acetic acid, propionic acid, butyric acid, and caproic acid during fermentative hydrogen production, the HDF obtained from pretreated mixed biomass were 18.1%-47.2% (Fig. 6c). Compared with the degradation of simple model compounds such as glucose (2.2%-6.8%) [28], the theoretical hydrogen production calculated through the VFAs production was much higher than the experimental data. This result suggested that the increases of VFAs just corresponded to the improvement of substrate degradation; the hydrogen production was not strictly positively related to the total VFAs production [14]. Such a phenomenon was more significant when mixed culture was applied to degrade complex actual biomass.

The mixture of RR and CP was mainly comprised of carbohydrates and proteins. For the degradation of carbohydrates, hydrogen could be produced via acetic acid and butyric acid pathways, while hydrogen could be also consumed via propionic and caproic acid pathways as well as homoacetogenic pathway [28]. Besides, previous studies found that almost no hydrogen was produced during the degradation of amino acids (derived from proteolysis) to VFAs [31]. Some types of bacteria may also utilise carbohydrates and proteins to produce VFAs without hydrogen production (or even

consuming hydrogen). Overall, these hydrogen unfavourable pathways were the main reason for the high HDF.

3.4. Carbon and energy conversion efficiencies

3.4.1. Carbon conversion efficiency

The CCE of RR and CP to VFAs and carbon dioxide during DF are as shown in Fig.

7a. The CCEs obtained from mono-fermentation of raw RR and CP were only 14.9% and 8.4%. When raw CP underwent hydrothermal acid pretreatment and then was used as the single fermentation substrate, the CCE slightly increased to 23.8%.

Pretreatment could improve the VFAs production due to the increase of solubilised organic matters. However the low biodegradable carbon sources in CP still led to a relatively low CCE. Co-fermentation of pretreated RR and CP could mitigate this unfavourable situation. With increasing the mix ratios from 1:1 to 25:1, the CCE significantly increased from 52.2% to 96.8%. In the case of sufficient nitrogen sources provided by CP, the addition of RR increased the bioavailable carbon sources, thereby improving the bioactivity of HPB. When pretreated RR was used as the single fermentation substrate, the high acetic acid (31.4 mM) and butyric acid (39.9 mM) concentrations (Table 3) resulted in a slight decrease of CCE (92.2%). Furthermore, most of the produced carbon was contained in acetic acid (12.2%-18.4%), butyric acid (19.3%-45.4%), and carbon dioxide (18.4%-27.5%), indicating that HPB mainly conducted acetic acid and butyric acid pathways.

3.4.2. Energy conversion efficiency

The ECE of RR and CP to hydrogen and VFAs during DF are shown in Fig. 7b. The

trends of ECE was similar to CCE. When raw biomass was used as the single fermentation substrate, the ECEs of RR and CP were only 11.2% and 7.6%, respectively. Pretreatment and co-fermentation could also remarkably improve the energy conversion. When pretreated RR was co-fermented with pretreated CP at the mix ratios of 1:1-25:1, the ECE increased from 41.4% to 90.8%. Notably, the hydrogen ECEs were only in the range of 6.3%-14.6% during co-fermentation. This suggested that a large portion of energy in RR and CP was transferred to the liquid phase and stored in the VFAs (35.1%-76.4%) especially in acetic acid (10.9%-17.1%) and butyric acid (21.5%-52.6%).

3.5. Comparison of energy conversion efficiencies during dark fermentation

A comparison of hydrogen yields and ECEs during DF between those in literature and in this study is shown in Table 4. Based on mono-fermentation, food waste generally contains large amounts of gelatinized starch derived from RR, steamed buns, and noodles [42]; these carbon sources are readily utilised by the HPB to produce hydrogen and VFAs. By contrast, the low content of biodegradable carbon sources in protein-rich microalgae may debilitate the bioaccessibility in the fermentation process, resulting in low hydrogen yields (around 20 mL/g VS) and ECEs (below 15%) [53].

Compared with mono-fermentation, co-fermentation of algae biomass (such as microalgae and macroalgae) or organic wastes (such as food waste, crude glycerol, and sewage sludge) can provide various ratios of nitrogen and carbon sources, thereby increasing the hydrogen yields (85.0-180.0 mL/g VS) and ECEs (34.2%-56.6%) during DF [25, 42, 53, 54]. RR as the main composition of food waste in China (more

than 30% of the total weight) is regarded as a suitable co-fermentation candidate due to its high bioavailability and biodegradability [15]. Additionally, the use of RR can avoid the inhibitory effects caused by the ubiquitous mineral compounds and high salinity embedded in food waste, as well as the high lipid content. In the present study, the hydrogen yield of 201.8 mL/g VS and the ECE of 71.0% obtained from mixed RR and CP showed significant improvements compared with other co-fermentation substrates. However these results were still lower than the values obtained from the mixture of simple model compounds (e.g., glucose and glutamic acid) [31].

For industrial application, the separation of bioavailable carbohydrate-rich organic matters from food waste would be beneficial for subsequent co-fermentation. Such a process requires good classification rules and disposal standards of food waste. Additionally, the low ECE of biohydrogen imply that DF may be considered as a biological pretreatment process for the downstream microbial factories, rather than a single gaseous biofuel production process. By combining with biomethane fermentation, the significant remaining energy in the VFAs can be more easily recovered, thereby enhancing the total ECE throughout the whole biorefinery process. Manzini et al. found that the produced VFAs were also potential raw materials for other biochemicals such as polyhydroxyalkanoate [3]. Thus, biohydrogen generation no longer would be the sole focus during DF. Further purification and utilisation of VFAs may be very beneficial in the future studies.

4 Conclusions

The mixtures of protein-rich microalgae and carbohydrate-rich rice residue could offer sufficient bioavailable carbon and nitrogen sources for dark fermentation. The optimised hydrothermal acid pretreatment for microalgae (140 °C, 10 min, 1% H₂SO₄, 75 g TS/L) and rice residue (140 °C, 10 min, 0.5% H₂SO₄, 50 g TS/L) could significantly improve the solubilisation and subsequent hydrogen and volatile fatty acids production. The organic fragments of raw rice residue and the spherical cells of raw microalgae were effectively disrupted into pieces and nanoparticles after pretreatment. The increasing presence of C=N group in the hydrolytic residues confirmed the strong interaction between sugar and amino acid. The occurrence of a special oxidation pattern at around 170-270 °C illustrated the presence of easily degraded fractions. When the pretreated rice residue and microalgae were co-fermented at a mix ratio of 5:1, the maximum hydrogen yield of 201.8 mL/g VS was achieved indicating a 10.7-fold increase compared with mono-fermentation of pretreated microalgae. Correspondingly, the maximum hydrogen production rate of 14.7 mL/g VS/h showed a 1.3-fold increase compared with mono-fermentation of pretreated rice residue. The produced energy after fermentation was mainly stored in hydrogen and volatile fatty acids, with a maximum energy conversion efficiency of 90.8%.

Acknowledgements

This work is supported by the National Science Foundation for Young Scientists of

China (No. 51606021), the International Cooperation and Exchange of the National Natural Science Foundation of China (No. 51561145013), the Fundamental Research Funds for the Central Universities (No. 106112017CDJPT140001), and the Venture & Innovation Support Program for Chongqing Overseas Returnees (No. cx2017019). Dr Richen Lin acknowledges the support from the European Union's Horizon 2020 research and innovation programme under the Marie Skłodowska-Curie grant agreement No. 797259. Prof Jerry D. Murphy is funded by Science Foundation Ireland (SFI) through the Centre for Marine and Renewable Energy (MaREI) under Grant No. 12/RC/2302.

References

- [1] Ghimire A, Frunzo L, Pirozzi F, Trably E, Escudie R, Lens PNL, et al. A review on dark fermentative biohydrogen production from organic biomass: Process parameters and use of by-products. *Appl Energ* 2015;144:73-95.
- [2] Palomo-Briones R, Razo-Flores E, Bernet N, Trably E. Dark-fermentative biohydrogen pathways and microbial networks in continuous stirred tank reactors: Novel insights on their control. *Appl Energ* 2017;198:77-87.
- [3] Manzini E, Scaglia B, Schievano A, Adani F. Dark fermentation effectiveness as a key step for waste biomass refineries: Influence of organic matter macromolecular composition and bioavailability. *Int J Energ Res* 2015;39(11):1519-27.
- [4] Cheah WY, Ling TC, Show PL, Juan JC, Chang JS, Lee DJ. Cultivation in wastewaters for energy: A microalgae platform. *Appl Energ* 2016;179:609-25.
- [5] Wiczorek N, Kucuker MA, Kuchta K. Fermentative hydrogen and methane production from microalgal biomass (*Chlorella vulgaris*) in a two-stage combined process. *Appl Energ* 2014;132:108-17.
- [6] Wu W, Wang PH, Lee DJ, Chang JS. Global optimization of microalgae-to-biodiesel chains with integrated cogasification combined cycle systems based on greenhouse gas emissions reductions. *Appl Energ* 2017;197:63-82.
- [7] Xia A, Cheng J, Song W, Su H, Ding L, Lin R, et al. Fermentative hydrogen production using algal biomass as feedstock. *Renew Sust Energ Rev* 2015;51:209-30.
- [8] Bundhoo MAZ, Mohee R, Hassan MA. Effects of pre-treatment technologies on dark fermentative biohydrogen production: A review. *J Environ Manage* 2015;157:20-48.
- [9] Mendez L, Mahdy A, Ballesteros M, González-Fernández C. Methane production of thermally pretreated *Chlorella vulgaris* and *Scenedesmus* sp. biomass at increasing biomass loads. *Appl Energ* 2014;129:238-42.
- [10] Xia A, Cheng J, Lin R, Liu J, Zhou J, Cen K. Sequential generation of hydrogen and methane from glutamic acid through combined photo-fermentation and methanogenesis. *Bioresour Technol* 2013;131:146-51.
- [11] Bundhoo MAZ, Mohee R. Inhibition of dark fermentative bio-hydrogen production: A review. *Int J Hydrogen Energ* 2016;41(16):6713-33.
- [12] Elbeshbishy E, Dhar BR, Nakhla G, Lee HS. A critical review on inhibition of dark biohydrogen fermentation. *Renew Sust Energ Rev* 2017;79:656-68.
- [13] Soltan M, Elsamadony M, Tawfik A. Biological hydrogen promotion via integrated fermentation of complex agro-industrial wastes. *Appl Energ* 2017;185:929-38.
- [14] Xia A, Cheng J, Ding L, Lin R, Song W, Zhou J, et al. Enhancement of energy production efficiency from mixed biomass of *Chlorella pyrenoidosa* and cassava starch through combined hydrogen fermentation and methanogenesis. *Appl Energ* 2014;120(120):23-30.
- [15] Sohu News. Food waste situation in China. <http://www.sohu.com/>; 2017 [accessed 24 Jan 2018].
- [16] Xia A, Cheng J, Murphy JD. Innovation in biological production and upgrading of methane and hydrogen for use as gaseous transport biofuel. *Biotechnol Adv* 2016;34(5):451-72.
- [17] Ghosh S, Chowdhury R, Bhattacharya P. Sustainability of cereal straws for the fermentative production of second generation biofuels: A review of the efficiency and economics of biochemical pretreatment processes. *Appl Energ* 2016;198:

- [18] Passos F, Uggetti E, Carrère H, Ferrer I. Pretreatment of microalgae to improve biogas production: A review. *Bioresour Technol* 2014;172:403-12.
- [19] Mendez L, Mahdy A, Timmers RA, Ballesteros M, González-Fernández C. Enhancing methane production of *Chlorella vulgaris* via thermochemical pretreatments. *Bioresour Technol* 2013;149(4):136-41.
- [20] Cheng J, Ding L, Lin R, Liu M, Zhou J, Cen K. Physicochemical characterization of typical municipal solid wastes for fermentative hydrogen and methane co-production. *Energy Convers Manage* 2016;117:297-304.
- [21] Rodríguez-Abalde Á, Gómez X, Blanco D, Cuetos MJ, Fernández B, Flotats X. Study of thermal pre-treatment on anaerobic digestion of slaughterhouse waste by TGA-MS and FTIR spectroscopy. *Waste Manage Res* 2013;31(12):1195-202.
- [22] Cheng J, Xia A, Song W, Su H, Zhou J, Cen K. Comparison between heterofermentation and autofermentation in hydrogen production from *Arthrospira (Spirulina) platensis* wet biomass. *Int J Hydrogen Energy* 2012;37(8):6536-44.
- [23] Walker M, Yue Z, Heaven S, Banks C. Potential errors in the quantitative evaluation of biogas production in anaerobic digestion processes. *Bioresour Technol* 2009;100(24):6339-46.
- [24] APHA. Standard methods for the examination of water and wastewater. American Public Health Association, American Water Works Association, Water Environment Federation, Washington, USA. 2005.
- [25] Xia A, Jacob A, Tabassum MR, Herrmann C, Murphy JD. Production of hydrogen, ethanol and volatile fatty acids through co-fermentation of macro- and micro-algae. *Bioresour Technol* 2016;205:118-25.
- [26] Ding L, Cheng J, Qiao D, Yue L, Li YY, Zhou J, et al. Investigating hydrothermal pretreatment of food waste for two-stage fermentative hydrogen and methane co-production. *Bioresour Technol* 2017;241:491-9.
- [27] Lay JJ, Lee YJ, Noike T. Feasibility of biological hydrogen production from organic fraction of municipal solid waste. *Water Res* 1999;33(11):2579-86.
- [28] Bakonyi P, Buitrón G, Valdez-Vazquez I, Nemestóthy N, Bédafi-Bakó K. A novel gas separation integrated membrane bioreactor to evaluate the impact of self-generated biogas recycling on continuous hydrogen fermentation. *Appl Energy* 2017;190:813-23.
- [29] Saady N. Homoacetogenesis during hydrogen production by mixed cultures dark fermentation: Unresolved challenge. *Int J Hydrogen Energy* 2013;38(30):13172-91.
- [30] Guo XM, Trably E, Latrille E, Carrère H, Steyer JP. Hydrogen production from agricultural waste by dark fermentation: A review. *Int J Hydrogen Energy* 2010;35(19):10660-73.
- [31] Xia A, Cheng J, Ding LK, Lin RC, Song WL, Su HB, et al. Substrate consumption and hydrogen production via co-fermentation of monomers derived from carbohydrates and proteins in biomass wastes. *Appl Energy* 2015;139:9-16.
- [32] Lin R, Cheng J, Murphy JD. Unexpectedly low biohydrogen yields in co-fermentation of acid pretreated cassava residue and swine manure. *Energy Convers Manage* 2017;151:553-61.
- [33] Lin R, Cheng J, Murphy JD. Inhibition of thermochemical treatment on biological hydrogen and methane co-production from algae-derived glucose/glycine. *Energy Convers Manage* 2018;158:201-9.
- [34] Brown MR, Jeffrey SW, Volkman JK, Dunstan GA. Nutritional properties of microalgae for mariculture. *Aquacult* 1997;151(1-4):315-31.
- [35] Girisuta B, Janssen LPBM, Heeres HJ. Green chemicals: A kinetic study on the conversion of

- glucose to levulinic acid. *Chem Eng Res Des* 2006;84(5):339-49.
- [36] Li H, Govind KS, Kotni R, Shunmugavel S, Riisager A, Yang S, et al. Direct catalytic transformation of carbohydrates into 5-ethoxymethylfurfural with acid-base bifunctional hybrid nanospheres. *Energy Convers Manage* 2014;88:1245-51.
- [37] Ramli NAS, Amin NAS. Optimization of renewable levulinic acid production from glucose conversion catalyzed by Fe/HY zeolite catalyst in aqueous medium. *Energy Convers Manage* 2015;95:10-9.
- [38] Toor SS, Rosendahl L, Rudolf A. Hydrothermal liquefaction of biomass: A review of subcritical water technologies. *Energy* 2011;36(5):2328-42.
- [39] Xia A, Cheng J, Lin R, Lu H, Zhou J, Cen K. Comparison in dark hydrogen fermentation followed by photo hydrogen fermentation and methanogenesis between protein and carbohydrate compositions in *Nannochloropsis oceanica* biomass. *Bioresour Technol* 2013;138(6):204-13.
- [40] Miller GL. Use of Dinitrosalicylic Acid Reagent for Determination of Reducing Sugar. *Anal Biochem* 1959;31(3):426-8.
- [41] Yilmaz Y, Toledo R. Antioxidant activity of water-soluble Maillard reaction products. *Food Chem* 2005;93(2):273-8.
- [42] Cheng J, Ding L, Lin R, Yue L, Liu J, Zhou J, et al. Fermentative biohydrogen and biomethane co-production from mixture of food waste and sewage sludge: Effects of physiochemical properties and mix ratios on fermentation performance. *Appl Energy* 2016;184:1-8.
- [43] Won SW, Choi SB, Yun YS. Performance and mechanism in binding of reactive orange 16 to various types of sludge. *Biochem Eng J* 2006;28(2):208-14.
- [44] Schwanninger M. Characterization of waste materials using FTIR spectroscopy: Process monitoring and quality assessment. *Spectrosc Lett* 2005;38(3):247-70.
- [45] Yaylayan VA, Kaminsky E. Isolation and structural analysis of maillard polymers: Caramel and melanoidin formation in glycine/glucose model system. *Food Chem* 1998;63(63):25-31.
- [46] Su J, Huang Z, Yuan X, Wang X, Li M. Structure and properties of carboxymethyl cellulose/soy protein isolate blend edible films crosslinked by Maillard reactions. *Carbohydr Polym* 2010;79(1):145-53.
- [47] Ross AB, Jones JM, Kubacki ML, Bridgeman T. Classification of macroalgae as fuel and its thermochemical behaviour. *Bioresour Technol* 2008;99(14):6494-504.
- [48] Gómez X, Cuetos MJ, Garc á AI, Mor án A. An evaluation of stability by thermogravimetric analysis of digestate obtained from different biowastes. *J Hazard Mater* 2007;149(1):97-105.
- [49] Su H, Cheng J, Zhou J, Song W, Cen K. Improving hydrogen production from cassava starch by combination of dark and photo fermentation. *Int J Hydrogen Energy* 2009;34(4):1780-6.
- [50] Lay JJ, Fan KS, Ku CH. Influence of chemical nature of organic wastes on their conversion to hydrogen by heat-shock digested sludge. *Int J Hydrogen Energy* 2003;28(12):1361-7.
- [51] Chen Y, Cheng J, Creamer K. Inhibition of anaerobic digestion process: A review. *Bioresour Technol* 2008;99(10):4044-64.
- [52] Lay CH, Sen B, Chen CC, Wu JH, Lee SC, Lin CY. Co-fermentation of water hyacinth and beverage wastewater in powder and pellet form for hydrogen production. *Bioresour Technol* 2013;135(3):610-5.
- [53] Ding L, Cheng J, Xia A, Jacob A, Voelklein M, Murphy JD. Co-generation of biohydrogen and biomethane through two-stage batch co-fermentation of macro- and micro-algal biomass. *Bioresour Technol* 2016;218:224-31.

[54] Silva FMS, Oliveira LB, Mahler CF, Bassin JP. Hydrogen production through anaerobic co-digestion of food waste and crude glycerol at mesophilic conditions. *Int J Hydrogen Energ* 2017;42:22720-9.

Lists of tables and figures

Table 1 Characteristics of rice residue pulp and *Chlorella pyrenoidosa* powder.

Table 2 Kinetic parameters of dark fermentation from pretreated rice residue and microalgae.

Table 3 Composition of volatile fatty acids in the dark fermentation effluents.

Table 4 Comparison of hydrogen yields and energy conversion efficiencies during dark fermentation among different studies.

Fig. 1 Technological processes and analytical parameters of co-fermentation from rice residue and microalgae.

Fig. 2 Effect of pretreatment parameters on organic matter solubilisation. The substrates used in (a), (b), (c) and (d) were rice residue, while the substrates used in (e), (f), (g), and (h) were microalgae.

Fig. 3 Changes of surface microstructures on rice residue and microalgae before and after pretreatment: (a) Rice residue without pretreatment; (b) Rice residue with hydrothermal pretreatment; (c) Rice residue with hydrothermal acid pretreatment (at 0.5% concentration); (d) Microalgae without pretreatment; (e) Microalgae with hydrothermal pretreatment; (f) Microalgae with hydrothermal acid pretreatment (at 1% concentration).

Fig. 4 Fourier transform infrared spectroscopy analysis of rice residue and microalgae before and after pretreatment: (a) Rice residue; (b) Microalgae.

Fig. 5 Derivative thermogravimetric analysis of rice residue and microalgae before

and after pretreatment: (a) Rice residue; (b) Microalgae.

Fig. 6 Hydrogen production via dark fermentation: (a) Hydrogen yield; (b) Hydrogen production rate; (c) Hydrogen discrepancy factor.

Fig. 7 Carbon and energy conversion efficiencies during dark fermentation: (a) Carbon conversion efficiency; (b) Energy conversion efficiency.

Table 1 Characteristics of rice residue pulp and *Chlorella pyrenoidosa* powder.

Parameters	Rice residue	<i>Chlorella pyrenoidosa</i>
Proximate analysis		
Moisture (wt%)	80.25 ± 2.38	5.96 ± 0.22
TS (wt%)	19.75 ± 2.38	94.04 ± 0.22
VS (wt%)	19.67 ± 0.00	79.83 ± 0.35
VS/TS (%)	99.61 ± 0.01	84.89 ± 0.32
Ultimate analysis		
C (VS%)	43.28 ± 0.00	50.19 ± 0.14
H (VS%)	6.01 ± 0.05	6.18 ± 0.34
O (VS%)	48.74 ± 0.02	33.14 ± 0.11
N (VS%)	1.69 ± 0.00	9.22 ± 0.07
S (VS%)	0.28 ± 0.02	1.27 ± 0.02
C/N molar ratio	29.81 ± 0.01	6.35 ± 0.03
Energy value (kJ/g VS)	16.92 ± 0.06	21.28 ± 0.39
tCOD (mg/g VS)	1124.59 ± 52.31	1439.63 ± 47.15
tCarbohydrates (mg/g VS)	913.76 ± 33.16	347.94 ± 16.35
tProteins (mg/g VS)	123.88 ± 14.27	480.86 ± 16.59
sCOD (mg/g VS)	26.31 ± 3.06	121.45 ± 7.86
sCarbohydrates (mg/g VS)	4.22 ± 0.95	54.31 ± 9.64
sProteins (mg/g VS)	12.55 ± 1.82	30.27 ± 6.13
Reducing sugars (mg/g VS)	1.91 ± 0.02	2.94 ± 0.36

The abbreviation referred to total (t) and solubilised (s) matters.

Table 2 Kinetic parameters of dark fermentation from pretreated rice residue and microalgae.

Mix VS ratios	Kinetic parameters				
	H _m (mL/g VS)	R _m (mL/g VS/h)	λ (h)	T _m (h)	R ²
1	93.1	11.5	5.36	8.34	0.9992
2.5	154.41	14.18	5.31	9.32	0.9998
5	200.48	15.97	5.59	10.21	0.9995
25	189.35	14.43	5.0	9.83	0.9972

Table 3 Composition of volatile fatty acids in the dark fermentation effluents.

Substrates	Volatile fatty acids (mM)				
	Acetic acid	Propionic acid	Butyric acid	Caproic acid	Total
Pure rice residue ^a	7.93 ± 1.86	/	2.87 ± 0.54	0.34 ± 0.02	11.14 ± 1.74
Pure microalgae ^a	9.46 ± 1.12	1.18 ± 0.07	2.55 ± 0.21	0.12 ± 0.01	13.32 ± 1.35
Pure rice residue ^b	31.44 ± 3.56	/	39.90 ± 4.06	1.80 ± 0.27	73.16 ± 3.71
Pure microalgae ^b	16.13 ± 2.03	3.15 ± 0.97	5.82 ± 1.15	0.77 ± 0.11	25.86 ± 1.76
Mixed biomass (VS ratio) ^b					
1	23.75 ± 2.99	0.84 ± 0.23	18.77 ± 1.56	1.13 ± 0.23	44.49 ± 2.52
2.5	28.32 ± 1.83	0.93 ± 0.01	29.05 ± 2.67	1.55 ± 0.41	59.81 ± 2.03
5	27.75 ± 3.46	0.74 ± 0.02	31.15 ± 3.12	1.75 ± 0.12	61.42 ± 3.09
25	33.34 ± 2.75	0.84 ± 0.16	41.17 ± 4.35	2.94 ± 0.57	78.30 ± 3.82

^a Raw biomass was used as the substrates during dark fermentation;

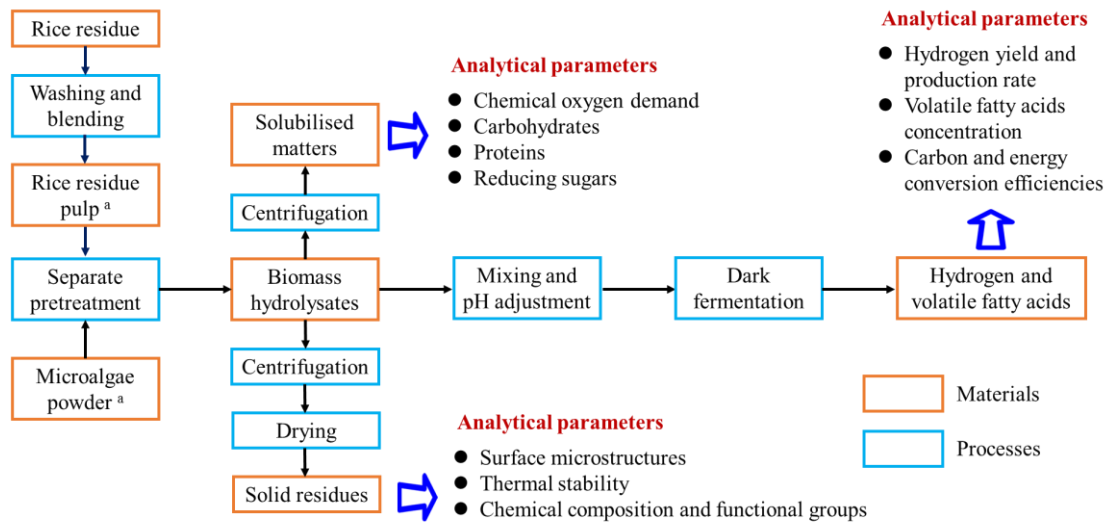
^b Hydrothermal acid pretreated biomass was used as the substrates during dark fermentation.

Table 4 Comparison of hydrogen yields and energy conversion efficiencies during dark fermentation among different studies.

Substrates	Optimal VS ratios	Specific H ₂ yields (mL/g VS)	Energy conversion efficiencies (%)	Ref.
<i>Chlorella pyrenoidosa</i>	/	18.3	13.8	[53]
<i>Nannochloropsis oceanica</i>	/	18.7	11.4	[53]
Food waste	/	149.3	49.5	[42]
Glucose + Glutamic acid	1:1	260.9	83.3	[31]
<i>Laminaria digitata</i> + <i>Arthrospira platenis</i>	9:1	85.0	54.5	[25]
<i>Laminaria digitata</i> + <i>Chlorella pyrenoidosa</i>	10.5:1	97.0	34.2	[53]
Food waste + crude glycerol	19:1 ^a	180.0	/	[54]
Food waste + sewage sludge	3:1	174.6	56.6	[42]
Rice residue + <i>Chlorella pyrenoidosa</i>	5:1	201.8	71.0	This study

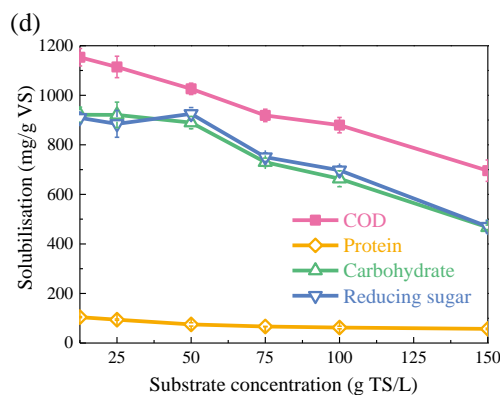
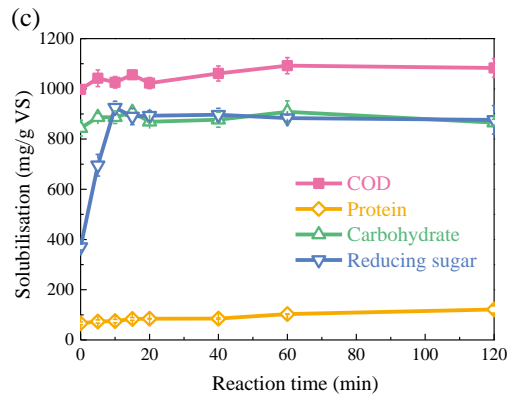
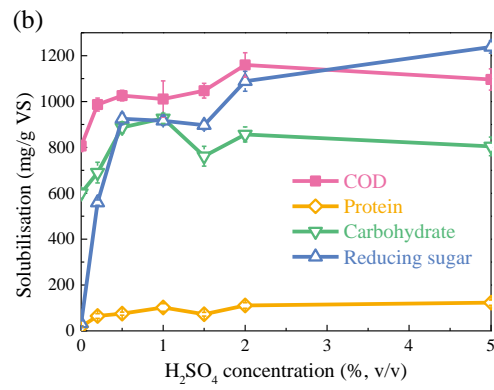
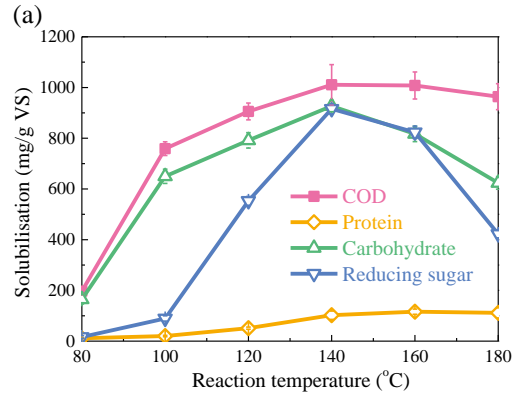
The inocula used in the dark fermentation were heat-pretreated anaerobic digestion sludge, and the fermentation temperature was 35 °C;

^a The volume ratio of food waste and crude glycerol;



^a In terms of raw biomass, the contents of moisture, total solids, volatile solids, and ash, as well as the total contents of chemical oxygen demand, carbohydrates, reducing sugars, and proteins, were also analysed.

Fig. 1 Technological processes and analytical parameters of co-fermentation from rice residue and microalgae.



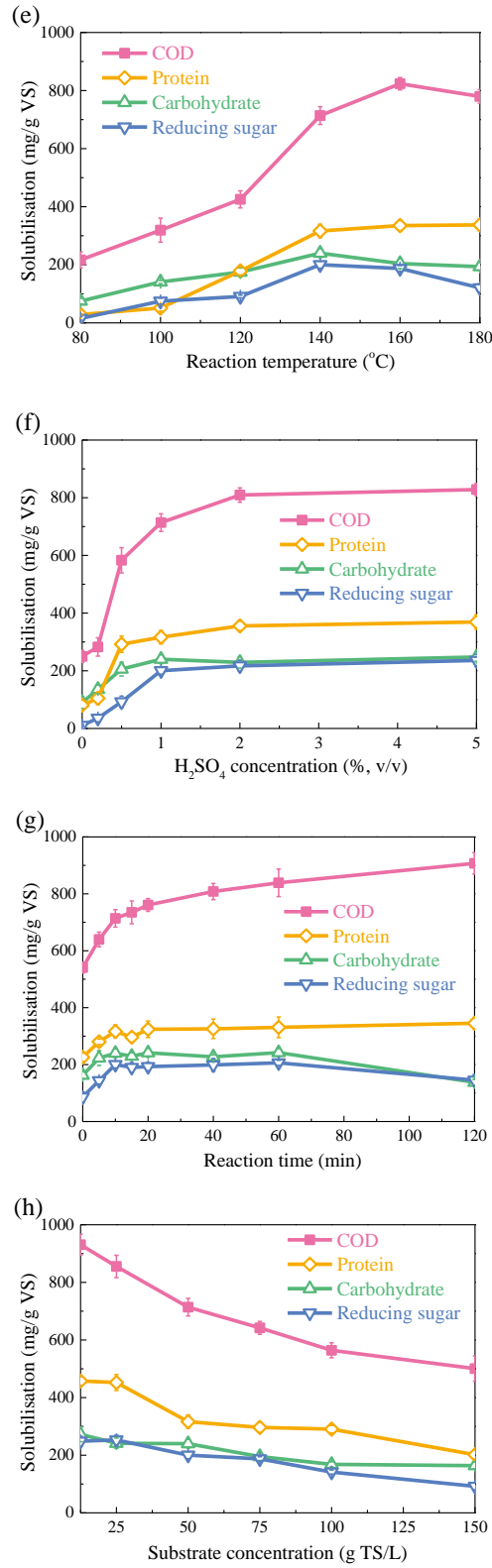


Fig. 2 Effect of pretreatment parameters on organic matter solubilisation. The substrates used in (a), (b), (c) and (d) were rice residue, while the substrates used in (e), (f), (g), and (h) were microalgae.

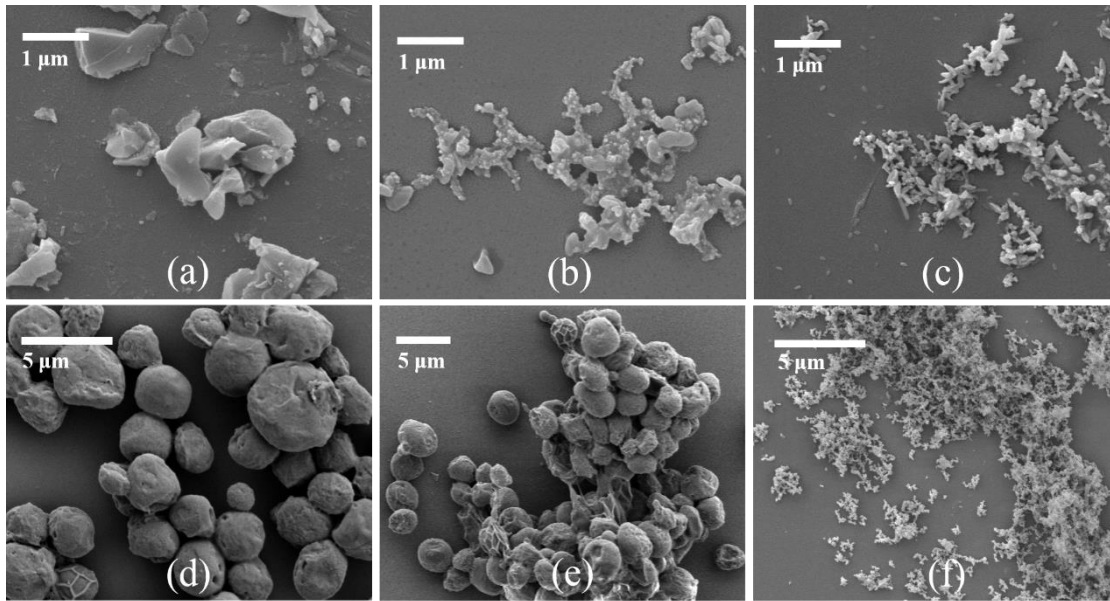


Fig. 3 Changes of surface microstructures on rice residue and microalgae before and after pretreatment: (a) Rice residue without pretreatment; (b) Rice residue with hydrothermal pretreatment; (c) Rice residue with hydrothermal acid pretreatment (at 0.5% concentration); (d) Microalgae without pretreatment; (e) Microalgae with hydrothermal pretreatment; (f) Microalgae with hydrothermal acid pretreatment (at 1% concentration).

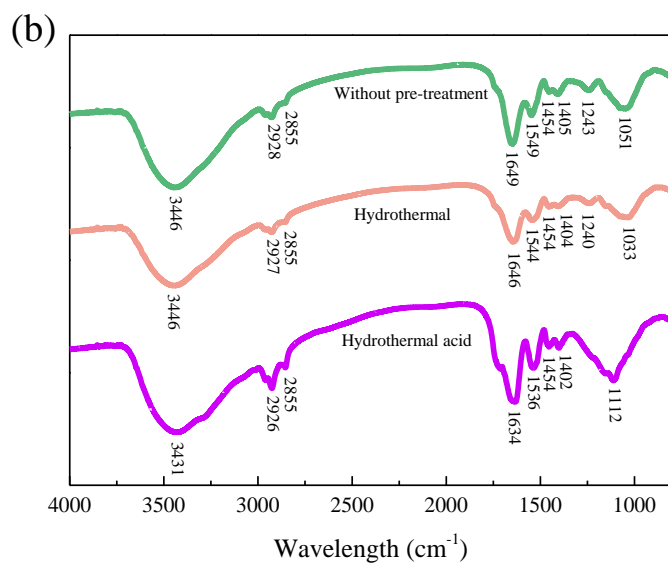
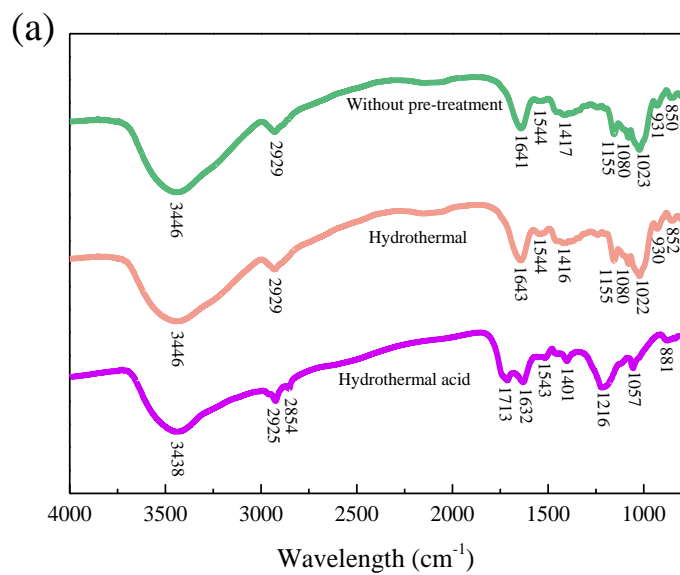


Fig. 4 Fourier transform infrared spectroscopy analysis of rice residue and microalgae before and after pretreatment: (a) Rice residue; (b) Microalgae.

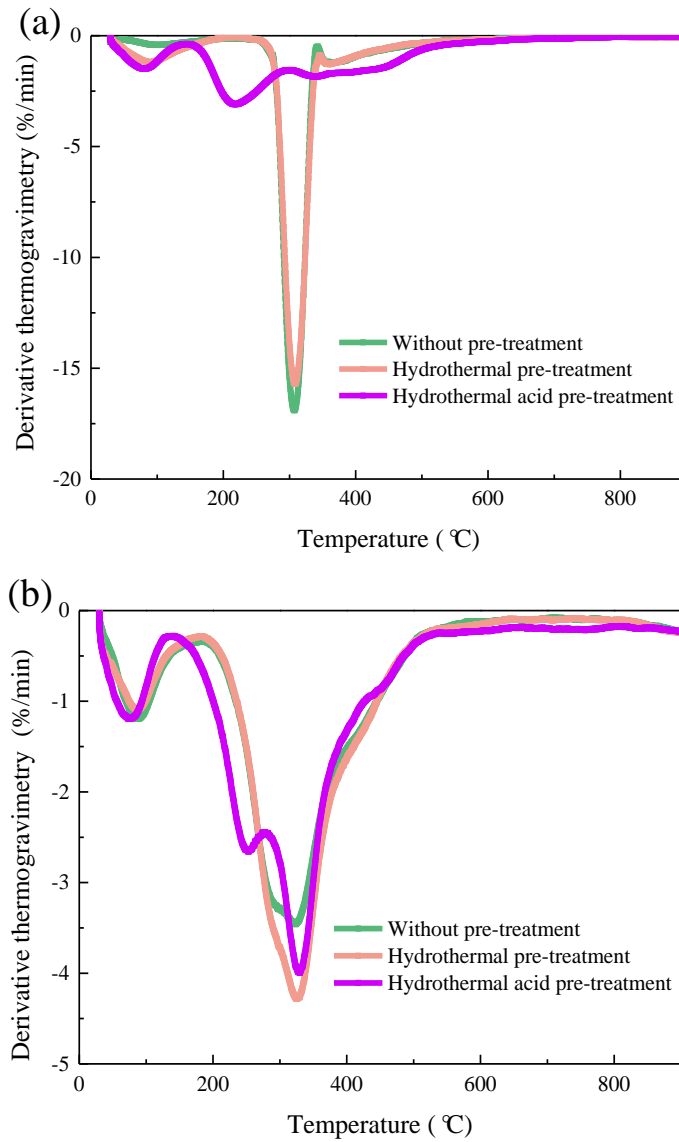


Fig. 5 Derivative thermogravimetric analysis of rice residue and microalgae before and after pretreatment: (a) Rice residue; (b) Microalgae.

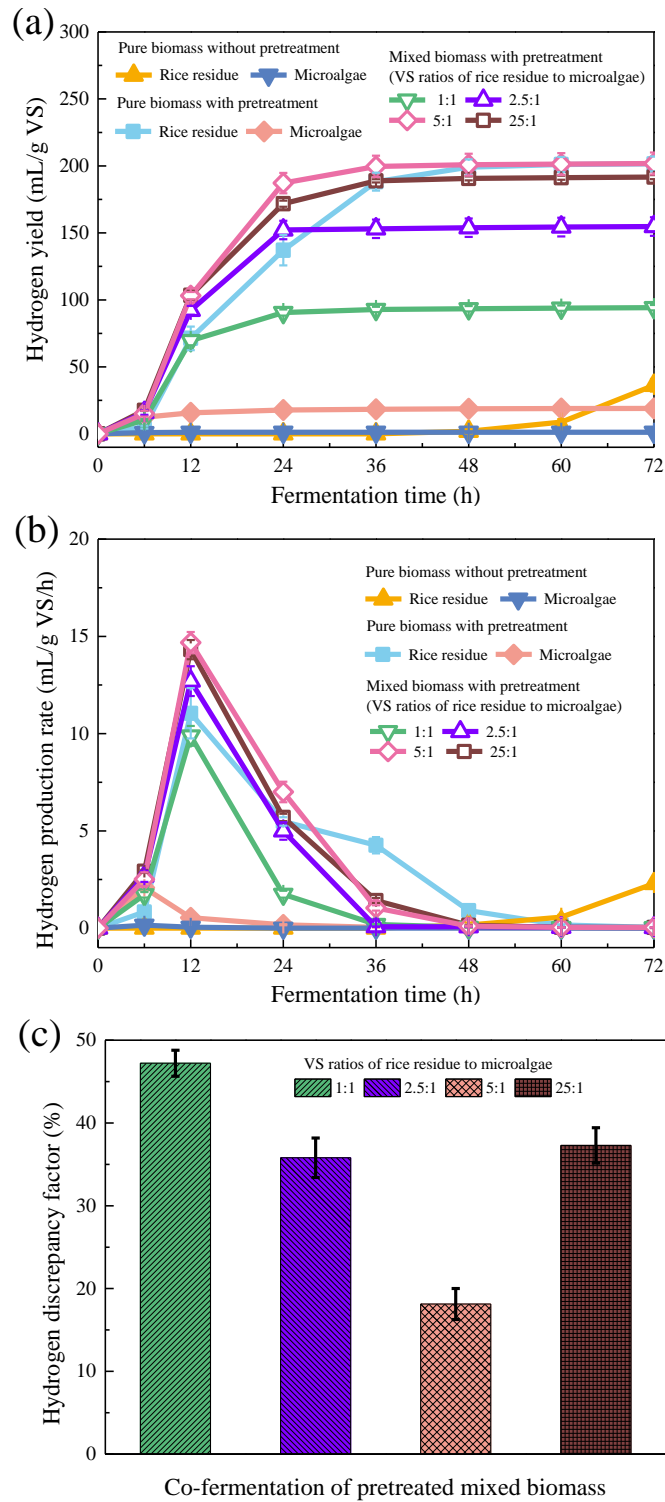


Fig. 6 Hydrogen production via dark fermentation: (a) Hydrogen yield; (b) Hydrogen production rate; (c) Hydrogen discrepancy factor.

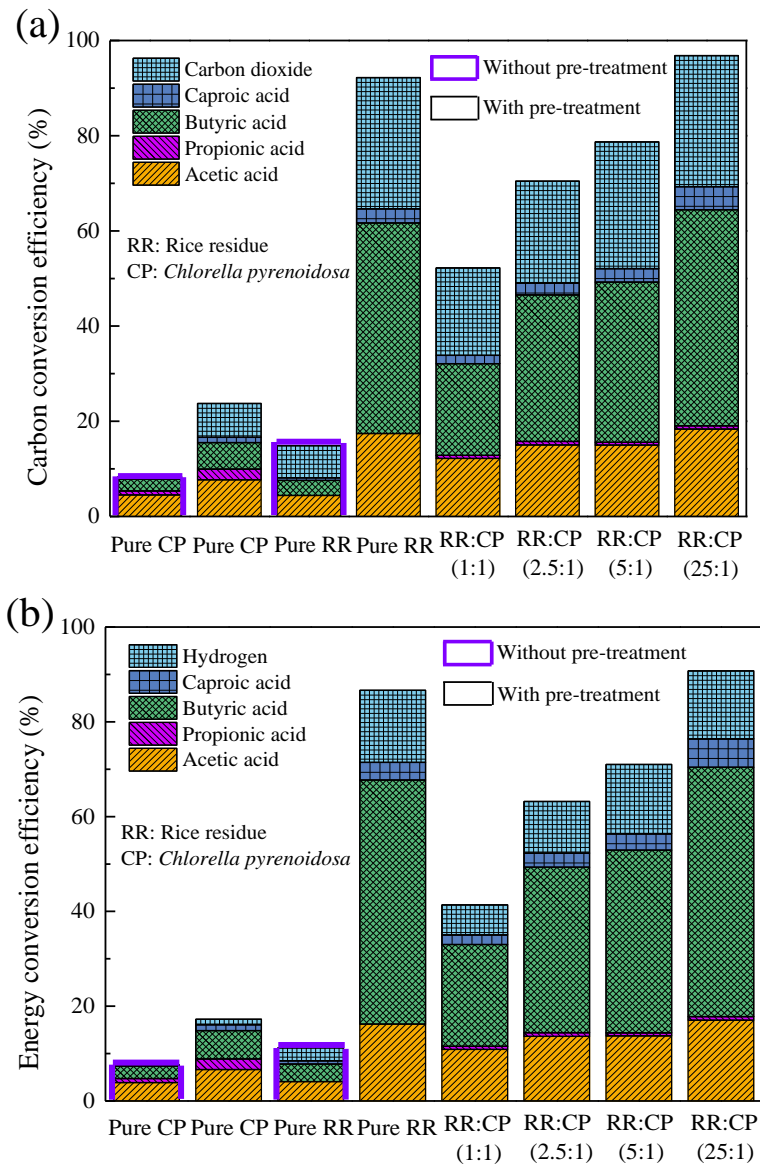


Fig. 7 Carbon and energy conversion efficiencies during dark fermentation: (a)

Carbon conversion efficiency; (b) Energy conversion efficiency.